

Topological features of atomic packings and the relation to glass-forming ability in metallic glass-forming systems

Yufei He(何宇飞), Jiaqi Wu(吴佳琦), and Maozhi Li(李茂枝)

Citation: Chin. Phys. B, 2026, 35 (**8**): 086101. DOI: 10.1088/1674-1056/ae1457
http://cpb.iphy.ac.cn; http://iopscience.iop.org/cpb

What follows is a list of articles you may be interested in

Optimization of glass-forming ability and synergistic enhancement of strength plasticity in $Cu_{50}Zr_{46}Al_4$ metallic glasses through Ag additions

Dongmei Li(李冬梅), Zhongyi Zhang(张忠一), Bolin Shang(尚博林), Rui Feng(丰睿), Xuefeng Li(李雪枫), and Peng Yu(余鹏)
Chin. Phys. B, 2025, 34 (**8**): 086107. DOI: 10.1088/1674-1056/adcea1

Atomic origin of minor alloying element effect on glass forming ability of metallic glass

Shan Zhang(张珊), Qingan Li(李庆安), Yong Yang(杨勇), and Pengfei Guan(管鹏飞)
Chin. Phys. B, 2025, 34 (**3**): 036105. DOI: 10.1088/1674-1056/ada756

Effect of Y element on atomic structure, glass forming ability, and magnetic properties of FeBC alloy

Jin-Hua Xiao(肖晋桦), Da-Wei Ding(丁大伟), Lin Li(李琳), Yi-Tao Sun(孙奕韬), Mao-Zhi Li(李茂枝), and Wei-Hua Wang(汪卫华)
Chin. Phys. B, 2024, 33 (**7**): 076101. DOI: 10.1088/1674-1056/ad3dd4

Heredity of clusters in the rapidly cooling processes of Al-doped $Zr_{50}Cu_{50}$ melts and its correlation with the glass-forming ability

Dadong Wen(文大东), Yonghe Deng(邓永和), Ming Gao(高明), and Zean Tian(田泽安)
Chin. Phys. B, 2021, 30 (**7**): 076101. DOI: 10.1088/1674-1056/abea93

Ab initio molecular dynamics study on the local structures in $Ce_{70}Al_{30}$ and $La_{70}Al_{30}$ metallic glasses

F X Li(李福祥), J B Kong(孔吉波), M Z Li(李茂枝)
Chin. Phys. B, 2018, 27 (**5**): 056102. DOI: 10.1088/1674-1056/27/5/056102

Topological features of atomic packings and the relation to glass-forming ability in metallic glass-forming systems

Yufei He(何宇飞), Jiaqi Wu(吴佳琦), and Maozhi Li(李茂枝)†

School of Physics and Key Laboratory of Quantum State Construction and Manipulation (Ministry of Education), Renmin University of China, Beijing 100872, *China*

(Received 16 September 2025; revised manuscript received 14 October 2025; accepted manuscript online 17 October 2025)

Molecular dynamics simulations were performed to study some model metallic glass-forming systems with distinct glass-forming ability (GFA), including monatomic metals and multicomponent alloys for understanding the physical origin of the GFA. Here the topological features of atomic packings in these systems were explored by employing the persistent homology (PH), a novel approach of computational algebraic topology to characterize the homology classes/Betti number and connection propensity of the densest packings. We found that the homology classes in all systems decrease with decreasing temperature, suggesting that the atomic packings generally become more and more heterogeneous during glass formation, but with different degrees. Moreover, we found that the connection propensity of the densest packings exhibits distinct evolution tendency in both multicomponent alloys and monatomic metals during cooling, and is consistent with the order of their GFA. This indicates that the connection propensity of the densest packings may be a general factor controlling the GFA of metallic glass-forming systems. Our findings demonstrate that the topological features of dense atomic packings in metallic glass-forming systems may be intrinsic in disordered structures and provide new insights into the structure-property relationship in glass-forming systems.

Keywords: glass-forming ability, persistent homology, molecular dynamics simulation

PACS: 61.43.Dq, 64.70.pe

DOI: 10.1088/1674-1056/ae1457 **CSTR:** 32038.14.CPB.ae1457

1. Introduction

Glasses are substances in far-from-equilibrium states, but commonly exist in nature and our daily life, including polymers, organics, silica glasses, metallic glasses, volcanic glass, amber glass,[1] and recently reported lunar glasses.[2] Glasses are often formed by vitrifying liquids if the cooling rate is high enough and crystallization is suppressed.[3] According to Kauzmann's hypothesis,[4] all liquids may be vitrified. As a matter of fact, the glass-forming ability (GFA) varies significantly with different glass-forming systems.[5] While polymers and silica glasses can be easily produced by cooling at a few kelvins per minute, the formation of metallic glasses (MGs) often requires much higher cooling rates of 10^2 K/s$\sim 10^6$ K/s.[5–7] Particularly, to vitrify the monatomic metals, the cooling rate is even as high as 10^{12} K/s$\sim 10^{14}$ K/s.[8,9] Therefore, GFA is a critical issue in the field of MGs, and its origin has stimulated broad scientific and technological interest. It has been well known that GFA of metallic alloys can be tuned by the constituent elements and compositions.[5] For instance, while Pd-based metallic alloys can be fabricated into bulk MGs with very slow cooling rates, Al-based MGs are obtained by relatively fast cooling rates.[10–12] Moreover, minor addition of some elements may significantly enhance GFA of metallic alloys.[13] However, further addition of a given element often deteriorates the GFA.[13] So far, the physical principles underlying alloying are still unclear. To design new and improved bulk MGs, a variety of empirical rules/parameters has been formulated based on various thermodynamic variables for predicting GFA of metallic alloys.[11,14–17] However, no single rule/parameter is able to fully capture the essential factors that influence GFA of most alloys. Meanwhile, great effort has been devoted to exploring the physical origin of GFA.[13–26] However, it is still an unresolved mystery and under hot debate.

So far, it is difficult to establish a direct link between the critical cooling rate and atomic structures/properties of metallic liquids and glasses, which makes the exploration of the physical origin of GFA a notoriously complex problem. To understand the physical origin of GFA, most studies have adopted a common strategy that one may characterize the atomic structure features or properties for different metallic alloys with distinct GFA and compare the observed differences, trying to establish a correlation between the observed differences and distinct GFA and elucidate its physical origin. It is generally believed that dense atomic packing associated with icosahedral short-range order (ISRO) may be quite important for enhancing GFA of metallic alloys, because ISRO with the five-fold symmetry and dense packing features may facilitate the geometric frustration and dynamic slowdown, favoring glass formation.[24,27–31] Therefore, numerous stud-

†Corresponding author. E-mail: maozhili@ruc.edu.cn

© 2026 Chinese Physical Society and IOP Publishing Ltd. All rights, including for text and data mining, AI training, and similar technologies, are reserved.

ies have been devoted to exploring the relationship between ISRO and GFA by analyzing the population of ISRO and its temperature evolution in various metallic glass-forming alloys with distinct GFA.[18,19] However, in some metallic glasses ISRO is not the dominant structure motif, and even absent.[32] Moreover, even if two different alloys share quite similar local atomic structures, their GFA may differ significantly.[33] A typical example is that while $Cu_{50}Zr_{50}$ and $Ni_{50}Al_{50}$ alloys are found to share quite similar local atomic structures in both supercooled liquid and glassy states characterized by Voronoi tessellation, both alloys exhibit distinct GFA.[33,34] Thus, it is unclear in what aspects dense atomic packings relate to the GFA in metallic glass-forming alloys. On the other hand, some studies show that GFA of CuZr metallic alloys is closely correlated with structural heterogeneity of the high-temperature liquid states, since it is better inherited by glassy states during glass formation of alloys with better GFA.[22] From the viewpoint of crystallization, computer simulations also suggest that the liquid-crystal interfacial structure may play an important role in the GFA of alloys, and chemical ordering may be crucial in determining interface tension in multicomponent alloys.[34,35]

Recent studies of monatomic MGs have drawn attention back to the role of dense atomic packing in GFA.[36] Because of the monatomicity, the glass formation of monatomic metallic liquids may be purely determined by the atomic packing, independent of chemical effects. For example, high-throughput physical vapor deposition produces various microregions with distinct packings of different atomic clusters in the vapor-deposited Ta film, indicating that proper packing of atomic clusters may be crucial for monatomic metallic liquids to form amorphous states.[36] Very recently, metallic glassy nanoparticles with diverse atomic arrangements have been successfully synthesized for monatomic FCC and HCP metals, but they demonstrated different stabilities.[9] Molecular dynamics simulations indicate that different stabilities of diverse nanoparticles are attributed to the difference in topological frustration degree induced by icosahedral-like clusters, suggesting that atomic packing may play an intrinsic role in determining the GFA of metallic alloys.[9] Therefore, to get more fundamental physical bases of GFA, it is vital to elucidate the atomic packing features in metallic glass-forming systems with different GFAs and how they influence GFA. Unfortunately, current atomic cluster analysis approaches based on the Voronoi tessellation fail to distinguish the specific atomic packing features or topological frustration in different metallic glass-forming systems.[35]

Recently, persistent homology (PH), a novel approach of computational algebraic topology to problems of feature detection and shape recognition in high-dimensional datasets,[37–39] has been widely applied in many fields such as social science, computing science, biology, and materials science.[37–43] In materials science, PH is introduced to extract topological structure features such as components, rings, and voids embedded in atomic configurations by treating the atoms as a three-dimensional (3D) point cloud in space, so that the topological fingerprints of atoms across scales and dimensions can be classified and visualized by persistent barcodes.[37–40,44] Therefore, it is advantageous to characterize the difference between materials structures.[41,45,46]

In this work, we employed PH to characterize the topological features of atomic packings, *i.e.*, homology classes or Betti numbers, and the connection propensity of the densest packings in metallic glass-forming systems. In order to elucidate the general topological features of atomic packings that are critical for the GFA, various metallic glass-forming systems with distinct GFA were adopted, including monatomic metals (Zr, Cu, Al, Ta), binary, and ternary alloys ($Ni_{50}Al_{50}$, $Cu_{50}Zr_{50}$, $Cu_{46}Zr_{46}Al_8$). We found that the evolution tendency of the topological atomic packings manifested by the graph filtrated PH is consistent with the order of GFA in multicomponent alloys during glass formation, suggesting that they may play an important role in the GFA. However, this is not the case in monatomic metals. Further analysis of the connection propensity of the densest packings by the assortativity coefficient reveals that its temperature evolution tendency is consistent with the order of the GFA in both multicomponent alloys and monatomic metals. This suggests that the connection propensity of the densest packings may be a general factor controlling the GFA of metallic glass-forming systems.

2. Model and method

2.1. Molecular dynamics simulations

In our studies, various metallic systems including monatomic metals (Zr, Cu, Al, Ta), binary and ternary alloys ($Ni_{50}Al_{50}$, $Cu_{50}Zr_{50}$, $Cu_{46}Zr_{46}Al_8$) were adopted. Classical molecular dynamics (MD) simulations were performed to generate the liquid and glass structures for the above metallic systems by using the large-scale atomic/molecular massively parallel simulator (LAMMPS) package.[47] The realistic embedded-atom method (EAM) potentials were applied to describe the interatomic interactions in these systems.[8,48–52] Each sample consists of 4000 atoms in a cubic box with periodic boundary conditions applied in three dimensions. For $Ni_{50}Al_{50}$, $Cu_{50}Zr_{50}$ and $Cu_{46}Zr_{46}Al_8$ alloy systems, the samples were firstly equilibrated at 2000 K for 2 ns, and then cooled down to 300 K with a cooling rate of 1.0×10^{12} K/s in the NPT ensemble. After that, the systems were further equilibrated at each temperature in the NPT ensemble with pressure adjusted to be zero. Finally, the samples were adequately relaxed in the NVT ensemble for more than 2 ns at each temperature, and 100 configurations were collected for structure

analysis. For monatomic metals, the samples were fully equilibrated at 5000 K, 4000 K, 2500 K, and 2000 K for Ta, Zr, Cu and Al, respectively, and 100 independent configurations were obtained for each system. These 100 configurations of each system were then cooled down to 100 K with a cooling rate of 1.0×10^{14} K/s in the NPT ensemble, outputting a configuration every 100 K for subsequent structural analysis.

2.2. Evaluation of glass-forming ability of monatomic metals

To characterize the GFA of the monatomic metals of Cu, Zr, Al, and Ta, we cooled the generated atomic configurations of each high-temperature liquid down to $0.1T_{\rm m}$ with cooling rates of 1.0×10^{12} K/s, 5.0×10^{12} K/s, 1.0×10^{13} K/s, and 1.0×10^{14} K/s, respectively. Here $T_{\rm m}$ denotes the melting temperature. The 10 independent configurations at $0.1T_{\rm m}$ in each system were generated. Here we used the bond-orientational order parameters to characterize the local structures of atoms in each configuration at $0.1T_{\rm m}$ and examined whether they are crystallized or not (see Section 1 in supplementary material).[35,53] Thus, the averaged fraction of crystallized atoms in 10 configurations can be used to evaluate the GFA of each monatomic metal. For the same cooling rate, a smaller fraction of crystallized atoms in a monatomic metal may refer to its relatively higher GFA (see supplementary material Fig. S1). For cooling rate of 1.0×10^{14} K/s, the fraction is about zero in all systems, indicating that the cooling rate is fast enough to suppress the crystallization in all monatomic metallic liquids. As cooling rate decreases to 1.0×10^{13} K/s, while the fraction is still zero in Ta and Cu, the fraction of crystallized atoms reaches more than 50% in Zr and a small fraction of atoms is crystallized in Al. With further decreasing cooling rate to 5.0×10^{12} K/s, the fraction keeps increasing in Al and Zr, but no crystallized atoms are detected in Ta and Cu. As cooling rate decreases to 1.0×10^{12} K/s, the fraction in Al and Zr liquids reaches almost 100%, and liquid Cu starts to crystallize, but the fraction in Ta is still almost zero. These results indicate that among Cu, Zr, Al, and Ta monatomic metals, Ta has the strongest GFA, followed by Cu, Al, and Zr successively.

2.3. Persistent homology

Since an atomic configuration obtained in MD simulations can be abstracted as a Delaunay network, *i.e.*, a simplicial complex, atoms and connections between two adjacent atoms can be regarded as vertices and edges, respectively. The topological features in this simplicial complex, *i.e.*, connected components can be analyzed by the PH via a filtration process.[37–39] Filtration can be conducted in several ways, each of which gives different descriptions of topological features.[37–39,54] In our work, a graph filtration based on edge weight was used,[55] because it is able to describe the topological features of atomic packing in short-to-medium range in disordered systems. Note that a Delaunay network only consists of vertices (0-dimensional simplex, 0-simplex) and edges between adjacent vertices (1-simplex), so that only zero-dimensional topological features were analyzed. To perform PH, a Delaunay network was first constructed for a liquid/glass structure via the radical Voronoi tessellation through Voro++ package,[56] so that the adjacent vertices and the length of each edge can be determined, with the edge length considered as the weight of the edge, as shown in Fig. 1(a). To perform the filtration process, each edge was added for two corresponding vertices in the network in order of the edge length from the shortest to the longest. In this process of adding an edge, a new connected component appears if any of the two corresponding vertices has not been connected to other adjacent vertices. If two independent connected components are connected together by adding a new edge, the connected component that appears late is merged into the one that appears early and disappears. Therefore, the filtration process is accompanied by the appearance and disappearance of a sequence of connected components (see Fig. S2). The corresponding weight at which a connected component appears/disappears is defined as its birth/death length scale. Thus, the persistence barcode of the connected components can be determined. Each bar corresponds to a homology class. The left and right points of each bar are the birth and death length scales, respectively, so that the bar length represents the persistent lifetime of each barcode, as illustrated in Fig. 1(b). The number of persistence bars represents the number of the homology classes in an atomic configuration, *i.e.*, Betti number.[44] Additionally, although there are some small surfaces obtained by Voronoi tessellation, eliminating these small faces or not does not affect the results in the filtration process. This is because each edge was added for two corresponding vertices (atoms) in the network in order of the edge length from the shortest to the longest, and small faces correspond to longer edges between two related atoms. Moreover, we tried to construct a Delaunay network for atomic configurations, so that the original Voronoi tessellation was used to fill the space without gaps or overlaps.

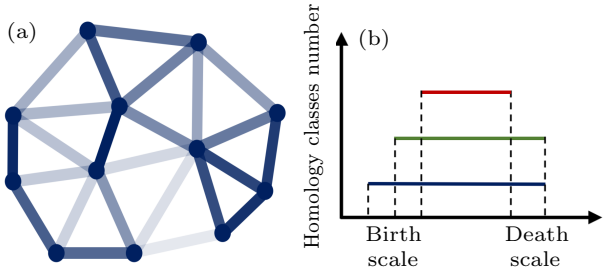


Fig. 1. Schematic diagram of a Delaunay network with vertices and edges (a), and persistent barcodes (b), respectively. The edge color in panel (a) represents its length.

Meanwhile, the minimum spanning tree of a Delaunay network can also be generated during the filtration process,[55]

which describes the densest packing as a skeletonized tree in disordered systems. The skeletonized tree can be obtained by retaining the edges that introduce new vertices to the global network or connect two different connected components during the filtration process[55] (see Sections S1 and S2 in the supplementary materials for more details).

3. Results

3.1. Persistent homology analysis of multicomponent glass-forming alloys

Figures 2(a)–2(i) show the persistent barcodes obtained by filtration of edge weight in $Cu_{50}Zr_{50}$, $Ni_{50}Al_{50}$, and $Cu_{46}Zr_{46}Al_8$ glass-forming liquids at three different temperatures, respectively. The profiles of the persistent barcodes are quite similar in $Cu_{50}Zr_{50}$ and $Cu_{46}Zr_{46}Al_8$ glass-forming liquids. However, $Ni_{50}Al_{50}$ glass-forming liquid exhibits a different barcode profile. In particular, the persistent lifetimes of the bars in three glass-forming alloys decrease significantly with decreasing temperature. While the number of the bars, *i.e.*, Betti number in $Cu_{50}Zr_{50}$ and $Cu_{46}Zr_{46}Al_8$ glass-forming liquids continuously decreases during cooling, it keeps almost unchanged in $Ni_{50}Al_{50}$ glass-forming liquid. For more details, we compared the distribution of the birth, death, and persistent length scales for $Cu_{50}Zr_{50}$, $Ni_{50}Al_{50}$, and $Cu_{46}Zr_{46}Al_8$ glass-forming liquids, respectively. As shown in Figs. 2(j) and 2(k), the distributions of birth and death scales in three systems are distributions with a single peak, and become narrower and higher with the peaks shifted to the larger scales as temperature decreases. Moreover, the distributions in $Cu_{50}Zr_{50}$ and $Cu_{46}Zr_{46}Al_8$ glass-forming liquids are much broader and larger, and the scales are also larger, in contrast to the narrower distributions and smaller scales in $Ni_{50}Al_{50}$ glass-forming liquid.

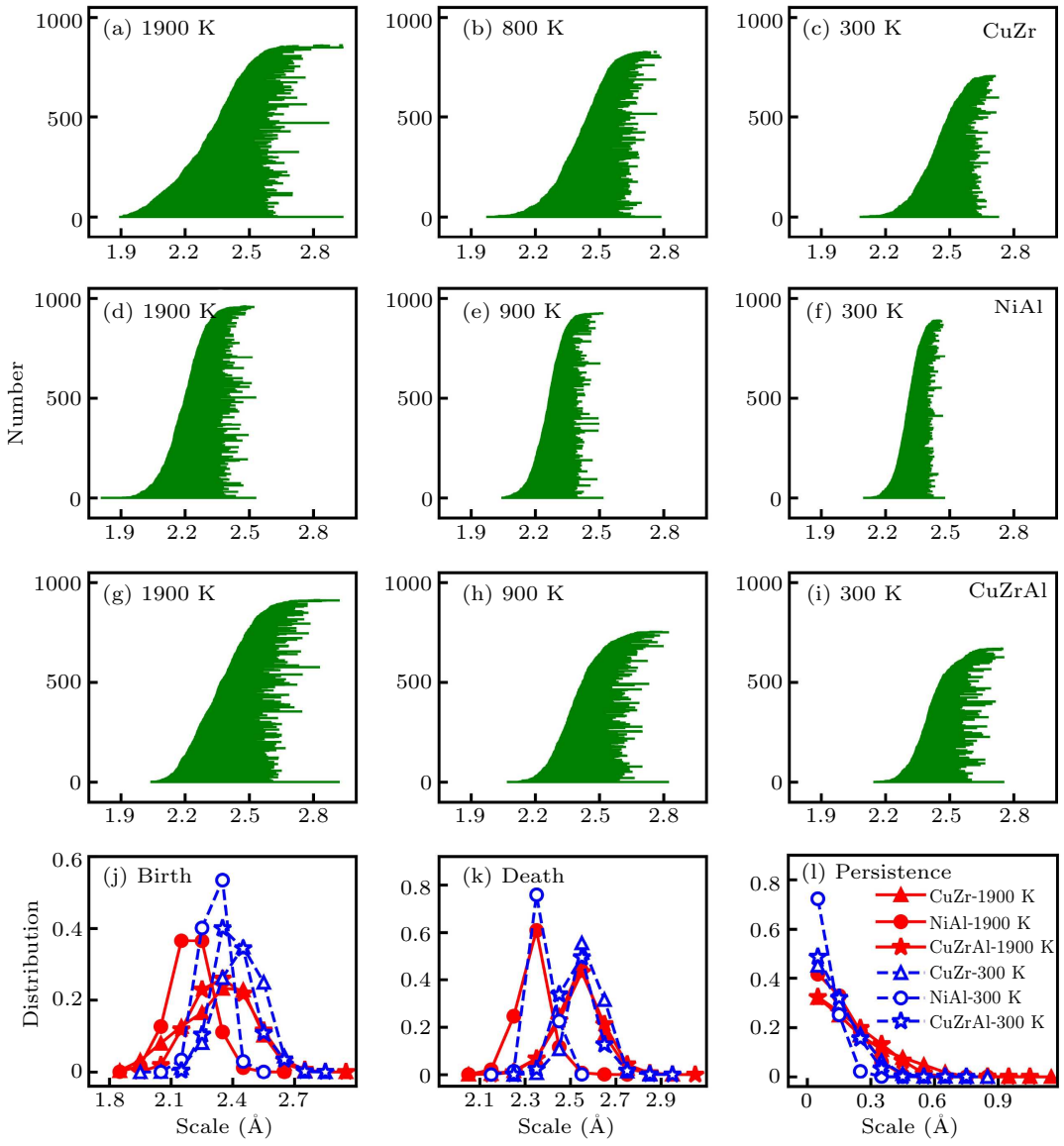


Fig. 2. (a)–(i) The number of persistent barcodes, *i.e.*, Betti number in $Cu_{50}Zr_{50}$, $Ni_{50}Al_{50}$, and $Cu_{46}Zr_{46}Al_8$ glass-forming liquids and glasses at three different temperatures, respectively. The distribution of birth (j), death (k), and persistence scale (l) of Betti number, respectively.

For the persistence scale, the distribution decreases monotonically as the scale increases, and becomes steeper with decreasing temperature in all three systems, as shown in Fig. 2(l). However, the distribution is much steeper in $Ni_{50}Al_{50}$ glass-forming liquid. These results indicate that the topological features of atomic packings in $Ni_{50}Al_{50}$ glass-forming liquid are quite different from those in $Cu_{50}Zr_{50}$ and $Cu_{46}Zr_{46}Al_8$ glass-forming liquids. The topological features in $Cu_{50}Zr_{50}$ and $Cu_{46}Zr_{46}Al_8$ glass-forming liquids are also slightly different. Therefore, the atomic structures of these three glass-forming liquids can be preliminarily distinguished from the topological atomic packing perspective. In addition, it also implies that the atomic structures in $Cu_{50}Zr_{50}$ and $Cu_{46}Zr_{46}Al_8$ glass-forming liquids may be more heterogeneous than those in $Ni_{50}Al_{50}$ glass-forming liquid.

To elucidate the evolution of the topological features of atomic packings during glass formation in these glass-forming systems, we investigated the temperature evolution of the homology classes, as shown in Figs. 3(a) and 3(b), respectively. While the number of homology classes continuously decreases in $Cu_{50}Zr_{50}$ and $Cu_{46}Zr_{46}Al_8$ glass-forming liquids in the whole cooling processes, it even increases slightly in $Ni_{50}Al_{50}$ glass-forming liquid during cooling and starts to decrease below glass transition temperature T_g. In addition, although the homology classes in $Cu_{46}Zr_{46}Al_8$ glass-forming liquids at high temperatures are more than those in $Cu_{50}Zr_{50}$ glass-forming liquid, they decrease more quickly and become less below T_g. Since each homology class represents a connected component of densely packed atoms, the change in the number of homology classes reflects the change of densely atomic packing regions. For $Cu_{50}Zr_{50}$ and $Cu_{46}Zr_{46}Al_8$ glass-forming liquids, the decrease in the number of homology classes indicates an increase in the scale of densely atomic packing regions during glass formation. Moreover, minor addition of Al may make the atomic packing more homogeneous in $Cu_{46}Zr_{46}Al_8$ liquid at high temperatures and greatly enhance the atomic packing evolution. For $Ni_{50}Al_{50}$ glass-forming liquid, however, the length scale of densely atomic packing regions represented by the number of homology classes increases a little in cooling process until T_g. The above findings indicate that the topological features in $Ni_{50}Al_{50}$ supercooled liquid states are quite similar to those in the high temperature liquid, whereas the topological features in $Cu_{50}Zr_{50}$ supercooled liquid states are significantly different from its high temperature liquid state during glass formation. The difference is more drastic in $Cu_{46}Zr_{46}Al_8$ glass-forming liquid. Thus, three glass-forming alloys exhibit distinct evolution tendency of the topological features of atomic packings during glass formation, which is consistent with the order of their GFA. The more drastically the number of homology classes decreases, the better the GFA is. More drastic evolution tendency may favor glass formation.

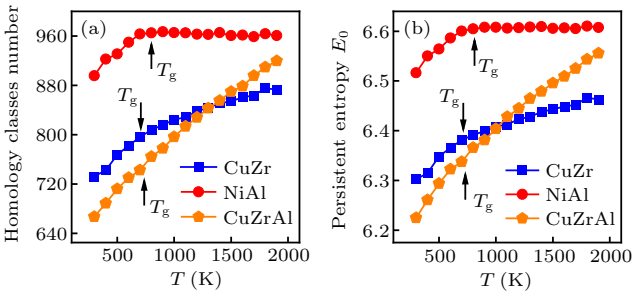


Fig. 3. Evolution of the number of homology classes (a) and persistent entropy (b) with temperatures in $Cu_{50}Zr_{50}$, $Ni_{50}Al_{50}$, and $Cu_{46}Zr_{46}Al_8$ glass-forming liquids during cooling, respectively.

To gain more insight into the topological features of atomic structures and their evolution during the cooling process in these glass-forming liquids, we characterized the ordering of homology classes in an atomic configuration by analyzing the persistent entropy defined as

$$S_{\mathrm{PH}} = -\sum_{j\in J}\left(\frac{l_j}{L}\right)\log\left(\frac{l_j}{L}\right), \tag{1}$$

where L is the sum of all values of the persistence, *i.e.*, length of bars, and l_j is the persistence of the j-th homology class, *i.e.*, the j-th bar.[57] The larger the persistent entropy value is, the more disordered the homology classes are, and *vice versa*. Figure 3(b) shows the evolution of persistent entropy with decreasing temperature during the cooling process in $Cu_{50}Zr_{50}$, $Ni_{50}Al_{50}$, and $Cu_{46}Zr_{46}Al_8$ glass-forming liquids, respectively. It can be seen that in each glass-forming liquid, the temperature-dependent behavior of the persistent entropy is quite similar to that of the number of homology classes. As temperature decreases, the persistent entropy of $Ni_{50}Al_{50}$ glass-forming liquid remains almost unchanged before glass transition, whereas it continuously decreases in $Cu_{50}Zr_{50}$ and $Cu_{46}Zr_{46}Al_8$ glass-forming liquids. This decrease is more pronounced in $Cu_{46}Zr_{46}Al_8$ glass-forming liquid. These results further indicate that $Ni_{50}Al_{50}$ glass-forming liquid maintains almost the same homology classes and ordering before glass transition. In contrast, however, the homology classes in $Cu_{50}Zr_{50}$ and $Cu_{46}Zr_{46}Al_8$ glass-forming liquids become more ordered and the topological features of the atomic packings continuously change during glass formation, deviating far away from those in high-temperature liquid states. This suggests that the atomic packings become more and more heterogeneous in $Cu_{50}Zr_{50}$ and $Cu_{46}Zr_{46}Al_8$ glass-forming liquids during glass formation. The minor addition of Al element causes an increase of homology classes in high-temperature liquid states of $Cu_{46}Zr_{46}Al_8$, leading to the increase of the persistent entropy. Moreover, it also causes a more drastic decrease of the persistent entropy in $Cu_{46}Zr_{46}Al_8$ glass-forming liquid during cooling, leading to smaller values at low temperatures, as shown in Fig. 3(b). This implies that the addition of Al makes the atomic packings more homogeneous in

$Cu_{46}Zr_{46}Al_8$ at high temperatures, compared to $Cu_{50}Zr_{50}$, and enhances the evolution of atomic heterogeneity in the rapid cooling process, leading to the most heterogeneous packings at low temperatures. The above results demonstrate the effectiveness of the persistent homology in capturing the differences in topological atomic packing among three glass-forming systems. Moreover, the evolution tendency of the topological atomic packing manifested by PH in glass formation is consistent with the order of the GFA in these three glass-forming systems.

3.2. Persistent homology analysis of monatomic metallic liquids

To examine the generality of the relation between persistent homology classes and GFA observed in binary and ternary metallic glass-forming alloys, we also analyzed the persistent barcodes for the monatomic metallic liquids of Ta, Cu, Al, and Zr at different temperatures, respectively. The profiles of the persistent barcodes at various temperatures and the distribution of birth, death, and persistence scales are different in these monatomic metallic liquids (see supplementary materials Fig. S4), indicating distinctive topological features of atomic packings in these monatomic metallic liquids. Figure 4 shows the evolution of the homology classes and persistent entropy with temperature in four monatomic liquids during cooling, respectively. Here the temperature is scaled by T_g. As shown in Fig. 4(a), the number of homology classes decreases with decreasing temperature, indicating an increase of the scale of topological atomic packings in monatomic liquids during glass formation. In liquid Cu, Al, and Ta, the temperature evolution of the number of the homology classes is relatively similar. The difference is that while the number in liquid Ta decreases more rapidly above $2T_g$, the number in liquid Al decreases more rapidly below T_g. Liquid Zr shows the largest number of homology classes overall, and the value decreases more rapidly below T_g. It can be seen that the evolution tendency of the number of homology classes in four monatomic systems does not show a correspondence to the order of their GFA. Figure 4(b) shows the temperature evolution of the persistent entropy in each monatomic liquid. The persistent entropy decreases with decreasing temperature in these monatomic metallic liquids, but exhibits some differences compared to the homology classes. The persistent entropy in liquid Cu, Zr, and Al shows different values, but similar temperature evolution behavior. However, the persistent entropy in liquid Ta drops drastically until $2T_g$, and further decreases gradually. It is evident that in four monatomic metallic systems the topological atomic packings characterized by PH do not show a consistency with the order of their GFA. However, we can still observe that the persistent entropy of these four monatomic metallic systems is generally higher than that of the multicomponent metallic glass-forming systems, indicating that the topological atomic packings in monatomic metallic systems are more homogeneous. Moreover, the persistent entropy decreases with temperature in all monatomic metallic liquids during cooling, leading to denser and more heterogeneous atomic packings.

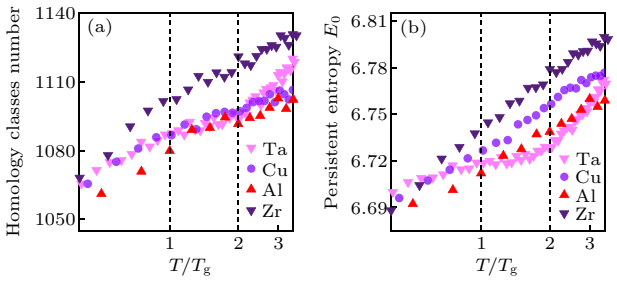


Fig. 4. Evolution of the number of homology classes (a) and persistent entropy (b) with temperature in monatomic metallic glass-forming liquids during cooling, respectively. The T/T_g is plotted on a logarithmic scale. The dashed lines mark the scales at T_g and $2T_g$.

3.3. Connection propensity of the densest packing: assortativity

To further elucidate the relation between persistent homology and GFA, we analyzed the connection propensity of the skeletonized tree of the Delaunay networks, *i.e.*, densest packings in these metallic glass-forming systems by calculating the assortativity coefficient defined as[58]

$$r = \frac{M^{-1}\sum_i j_i k_i - \left[M^{-1}\sum_i \frac{1}{2}(j_i + k_i)\right]^2}{M^{-1}\sum_i \frac{1}{2}(j_i^2 + k_i^2) - \left[M^{-1}\sum_i \frac{1}{2}(j_i + k_i)\right]^2}, \tag{2}$$

where M is the number of edges in the skeletonized tree, and j_i and k_i are the degrees of vertex j and vertex k connected by edge i. The degree of a vertex is the number of edges connected to it. The assortativity coefficient values are located in the range of -1 and 1. $r = -1$ and 1 correspond to the most disassortative mixing of connected vertices with significantly different degrees and the most assortative mixing of connected vertices with almost the same degrees, respectively, and $r = 0$ refers to the random mixing. The assortativity coefficient describes the similarity of the local close-packed environments of two connected atoms. While assortative mixing means that atoms with similar close-packed environments tend to connect to each other, disassortative mixing means that atoms with different close-packed environments tend to connect together. Random mixing means that there is no preference in the connection of atoms. The assortativity coefficient characterizes the packing heterogeneity from the perspective of the connection propensity of local atomic closed packings.

Figure 5 shows the evolution of the assortativity coefficient values with temperature scaled by T_g in the cooling process in these metallic glass-forming liquids. It can be seen in Fig. 5(a) that the skeletonized trees in binary and ternary glass-forming alloys have negative assortativity coefficient values,

indicating the disassortative mixing properties. However, the skeletonized trees in these glass-forming alloys exhibit quite different mixing properties. As shown in Fig. 5(a), the assortativity coefficient values in $Ni_{50}Al_{50}$ glass-forming liquid remain nearly constant above T_g and decrease a little below T_g. In contrast, the assortativity coefficient in $Cu_{50}Zr_{50}$ glass-forming liquid decreases significantly with decreasing temperature, becoming more negative. In the $Cu_{46}Zr_{46}Al_8$ system, the assortativity coefficient presents the most significant decrease as the temperature decreases, starting from the highest value and reaching the lowest value in the glass state among the three systems. This suggests that the connection propensity of the skeletonized trees in $Ni_{50}Al_{50}$ glass-forming liquids does not change in supercooled liquid states, remaining the same as that in high-temperature liquid states. However, the atomic packing propensity exhibits a continuous increase in the disassortative mixing feature during the glass formation process in $Cu_{50}Zr_{50}$ and $Cu_{46}Zr_{46}Al_8$ glass-forming liquids. The evolution tendency of the disassortative mixing feature is consistent with the order of GFA in these metallic glass-forming alloys.

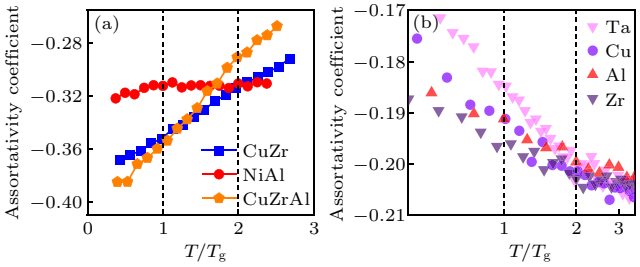


Fig. 5. Evolution of the assortative coefficient in alloy systems (a) and in monatomic systems (b). The solid lines in panel (b) represent the fitted assortativity coefficient in supercooled liquid state, and the T/T_g in panel (b) is plotted on a semi-log plot.

In the following, we also analyzed the temperature evolution of the assortativity coefficient for the connection propensity of the skeletonized tree of the Delaunay networks in these monatomic metallic liquids. As shown in Fig. 5(b), assortativity coefficients are less negative than those in multicomponent metallic systems, indicating that the atomic packings prefer less disassortative mixing in monatomic metallic systems. Moreover, the assortativity coefficients increase with decreasing temperature. This indicates that atomic connection propensity in monatomic metallic systems tends to become less and less disassortative mixing in glass formation, in contrast to that in multicomponent metallic systems shown in Fig. 5(a). In monatomic systems, the distribution of the persistence scale becomes steeper with decreasing temperature (see supplementary materials Fig. S4(o)), but the number of persistent barcodes does not change much (see Fig. 4(a)). This implies that topological features in atomic packings become similar during cooling in a monatomic liquid. Therefore, the connection propensity of the densest packings becomes less disassortative mixing during cooling in monatomic systems. In multicomponent alloys, however, the opposite temperature dependence of the assortativity coefficient could result from the chemical effect, which will be discussed in the next section.

It can also be seen that the assortativity coefficient increases more rapidly in liquid Ta, followed sequentially by liquid Cu, Al, and Zr (see Fig. S5 in supplementary materials). The increasing tendency is also consistent with the order of their GFA. Thus, the atomic connection propensity of the skeletonized tree of the Delaunay networks may be an intrinsic factor that generally correlates to the GFA in metallic glass-forming systems.

Note that the assortativity coefficients in $Cu_{50}Zr_{50}$ and $Cu_{46}Zr_{46}Al_8$ glass-forming liquids show a crossover at around $2T_g$, below which they decrease more rapidly. However, $Ni_{50}Al_{50}$ glass-forming liquid does not show such a crossover behavior around $2T_g$. For monatomic metallic liquids, the assortativity coefficient in liquid Ta and Zr exhibits a crossover at around $2T_g$ (see Fig. S5). Moreover, the assortativity coefficient in liquid Ta also shows a crossover at around T_g. However, the assortativity coefficient in liquid Cu and Al does not exhibit an obvious crossover behavior during cooling. The crossover behavior may be system dependent. It is not clear whether it is related to the GFA or dynamic properties in metallic glass-forming systems or not.

4. Discussion

4.1. Correlation between topological atomic packings and GFA

Based on the above analysis, it is clear that the connection propensity of the densest packings characterized by the assortativity coefficient may be a general factor controlling the GFA of metallic glass-forming systems. For multicomponent metallic alloys, the connection propensity tends to be more disassortative mixing during cooling, and the evolution tendency is consistent with the order of the GFA. The more disassortative mixing the connection propensity is, the better the GFA is. For monatomic metals, the connection propensity tends to become less disassortative mixing during cooling, and the evolution tendency is also consistent with the order of their GFA. The less disassortative mixing the connection propensity is, the better the GFA is. Therefore, the connection propensity of the densest packings, *i.e.*, assortativity, should be the intrinsic factor that generally controls the GFA in metallic glass-forming systems. For the topological atomic packings manifested by the homology classes/persistent entropy, while their evolution tendency is consistent with the order of GFA in the multicomponent alloys, it is not the case in the monatomic metallic systems. However, the homology classes/persistent

entropy decreases with decreasing temperature in both multicomponent and monatomic metallic systems, leading to denser and more heterogeneous atomic packings of the Delaunay networks.

The correlation between the topological atomic packings and GFA of metallic glass-forming systems can be generally understood from the perspective of heredity. As shown in Fig. 5, the assortativity coefficients in both multicomponent and monatomic metallic glass-forming systems deviate from the values of their high-temperature liquid states during glass formation, and the deviation degree is consistent with the order of the GFA. The deviation means to what degree the topological features of the high-temperature liquids are inherited into supercooled and even glassy states during glass formation. Thus, systems with poorer GFA tend to inherit the topological features of their high-temperature liquids into the supercooled liquids and glassy states, whereas those with better GFA tend to develop more and more densely packed networks during cooling, deviating substantially from their high-temperature liquid states. The more the assortativity coefficient value deviates from the high-temperature value, the better the GFA is. In $Ni_{50}Al_{50}$ glass-forming liquid, the persistent entropy and the assortativity coefficient keep almost unchanged above T_g, as shown in Figs. 3(b) and 5(a), respectively, and almost no deviation occurs before glass transition. This suggests that almost all topological features of PH and the connection propensity of the densest packings in the high-temperature liquid state are inherited into the supercooled states. In contrast, the persistent entropy and the assortativity coefficient in $Cu_{46}Zr_{46}Al_8$ glass-forming liquid decrease continuously in the cooling process, deviating significantly away from the high-temperature values. This indicates that fewer and fewer topological features of PH and the connection propensity of the densest packings in the high-temperature liquid state are inherited into the supercooled states, and even glassy states during cooling.

4.2. Evolution of the Voronoi entropy in metallic liquids during glass formation

As mentioned above, $Cu_{50}Zr_{50}$ and $Ni_{50}Al_{50}$ glass-forming liquids are found to share quite similar local atomic structures, but have distinct GFA.[33] This indicates that the atomic structures characterized by Voronoi tessellation cannot correlate to the GFA. To further demonstrate the key role of topological atomic packings in GFA in metallic glass-forming systems, we also analyzed the temperature evolution of the atomic structure characterized by Voronoi tessellation in terms of the Voronoi entropy defined as[59]

$$S_V = -\sum_{j=1}^{N_V} p_j \log p_j,$$

where p_j represents the fraction of Voronoi polyhedron type j in an atomic configuration, and N_V denotes the number of Voronoi polyhedral types. If p_j is 1 and the probability of all other types of polyhedra is 0, then $S_V = 0$, which indicates that the system is in the most ordered structure configuration. However, if all polyhedral types have the same probability of $1/N_V$, S_V will get its maximum value, which indicates that the atomic configuration is most disordered. Since the Voronoi entropy can quantify the diversity of atomic structures and the configurational entropy, it has been considered as a universal metric to capture the structural evolution in glass transition.[59,60] Figure 6 shows the temperature evolution of Voronoi entropy in monatomic, binary and ternary metallic glass-forming liquids during fast cooling, respectively. For multicomponent glass-forming alloys, the smaller the Voronoi entropy is, the better the GFA, which can be clearly seen in glassy states, as shown in Fig. 6(a). However, it is not the case for monatomic liquids. Among these monatomic liquids, liquid Ta is the best glass-former, and its Voronoi entropy is the smallest. For liquid Cu and Zr, the Voronoi entropy values are quite close in whole cooling process, as shown in Fig. 6(b), but their GFA differs significantly (see supplementary materials Fig. S1). The Voronoi entropy of liquid Al changes the least during cooling, but its GFA is not the weakest. Therefore, the Voronoi entropy values of these monatomic liquids are not consistent with the order of their GFA. Therefore, the temperature evolution of the Voronoi entropy does not show universal correlation between atomic structures and GFA in both multicomponent and monatomic metallic glass-forming systems. On the other hand, although the Voronoi entropy values in the glassy states of the multicomponent glass-forming alloys are consistent with the order of their GFA, the difference in the Voronoi entropy values is very small, especially for $Ni_{50}Al_{50}$ and $Cu_{50}Zr_{50}$ systems. Such a small difference is difficult to account for their distinct GFA.[34,35]

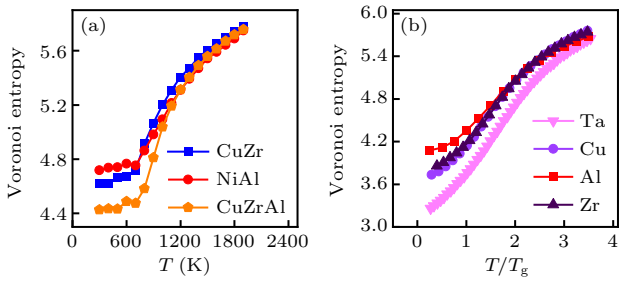


Fig. 6. Evolution of the Voronoi entropy with temperature in cooling process in binary & ternary (a) and monatomic (b) metallic glass-forming liquids, respectively.

4.3. Effect of chemical ordering on persistent homology in multicomponent metallic glass-forming liquids

The above results indicate that the assortativity properties become more disassortative mixed during cooling in multicomponent glass-forming alloys, while they become more assortative mixed in monatomic metallic liquids. This could be due to the chemical effect. To elucidate it, we analyzed how

the chemical short-range order (CSRO) influences the assortativity in multicomponent glass-forming systems. Here the Warren–Cowley parameter was employed to characterize the CSRO for each atom[61]

$$\alpha_{AB} = 1 - \frac{Z_{AB}}{\chi_B Z_A},$$

where Z_{AB} is the partial coordination number (CN) (B atoms) around atom A, Z_A is the CN around A, and χ_B is the nominal composition of B. Different α_{AB} reflect different chemical environments. A negative α_{AB} means the preferential coordination between A and B elements, whereas a positive α_{AB} means the non-preferential coordination between A and B elements. Figure 7(a) shows the temperature evolution of CSRO in $Cu_{50}Zr_{50}$, $Ni_{50}Al_{50}$ and $Cu_{46}Zr_{46}Al_8$ glass-forming liquids, and similar behavior can be observed. The CSRO in $Ni_{50}Al_{50}$ glass-forming liquid decreases more slowly with decreasing temperature. This is consistent with previous studies.[33]

Figure 7(b) shows the temperature evolution of atomic average degree of skeletonized trees during the cooling process. It is noted that for the generation of the minimum spanning tree in multicomponent systems, the distance between small atoms and other atoms is shorter compared to the distance between large atoms and other atoms, making it easier for small atoms to form larger degrees. The results also show that atomic degree decreases for large atoms and increases for small atoms during the cooling process, but this trend is not obvious in $Ni_{50}Al_{50}$. The growing preferential coordination between the different types of atoms in the cooling process indicates that atoms with different degrees tend to connect together, as shown in Fig. 7(a). Therefore, the preference in the chemical ordering may be related to the decrease in the assortativity coefficients in multicomponent systems. In multicomponent alloys, the development of chemical short-range order during cooling promotes the preferential connection between atoms with different sizes or types, leading to more disassortative mixing, which may enhance the topological frustration, thus favoring glass formation. On the other hand, in monatomic metallic systems the closest-packed skeletonized tree presents a reduction of disassortative mixing and prefers the random mixing during glass formation, reflecting the most intrinsic atomic packing features in glass formation. These findings also suggest that chemical ordering has a great impact on the topological features of atomic packings in multicomponent metallic glass-forming alloys.

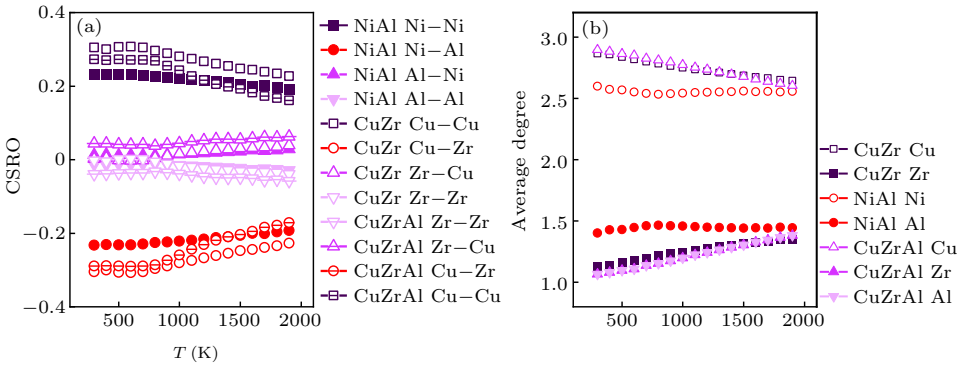


Fig. 7. Evolution of the average Warren–Cowley parameter (a) and the average degree of skeletonized trees (b) with temperature during cooling process in $Cu_{50}Zr_{50}$, $Ni_{50}Al_{50}$, and $Cu_{46}Zr_{46}Al_8$ metallic glass-forming liquids.

5. Conclusion

In this work, we employed the PH via graph filtration to explore the topological features of atomic packings and their temperature evolution in various model metallic glass-forming systems with distinct GFA. We found that the PH can effectively characterize the topological features of atomic packings and capture the differences in different metallic glass-forming systems. Our results demonstrate that the connection propensity of the densest packings may be a general factor controlling the GFA of metallic glass-forming systems. For multicomponent metallic glass-forming alloys, the topological atomic packings manifested by the graph filtrated PH may also play an important role in the GFA. Our results also suggest that the correlation between the topological atomic packings and GFA of metallic glass-forming systems can be generally understood from the perspective of heredity. Systems with poorer GFA tend to inherit the topological features of their high-temperature liquids into the supercooled liquids and glassy states, whereas those with relatively better GFA tend to develop more and more densely packed networks during cooling, deviating drastically from their high-temperature liquid states. The above structure features cannot be revealed by Voronoi tessellation-based atomic cluster analysis approaches. These findings shed light on the structural analysis in metallic glass-forming systems from the perspective of topology and provide new understandings for the structure-property relationship.

Acknowledgements

Computational resources were provided by the Physical Laboratory of High-Performance Computing at Renmin Uni-

versity of China.

Project supported by the National Natural Science Foundation of China (Grant Nos. 52031016 and 12574220).

References

[1] Berthier L and Ediger M D 2016 *Phys. Today* **69** 40
[2] Chen Z, Zhao Y, Chi X, Yan Y, Shen J, Zou M, Zhao S, Liu M, Yao W, Zhang B, Ke H, Ma X L, Bai H, Yang M, Zou Z and Wang W H 2023 *Sci. Adv.* **9** eadi6086
[3] Debenedetti P G and Stillinger F H 2001 *Nature* **410** 259
[4] Kauzmann W 1948 *Chem. Rev.* **43** 219
[5] Wang W H, Dong C and Shek C H 2004 *Mater. Sci. Eng. R* **44** 45
[6] Klement W, Willens R H and Duwez P 1960 *Nature* **187** 869
[7] Nishiyama N, Takenaka K, Miura H, Saidoh N, Zeng Y and Inoue A 2012 *Intermetallics* **30** 19
[8] Zhong L, Wang J, Sheng H, Zhang Z and Mao S X 2014 *Nature* **512** 177
[9] Tong X, Zhang Y E, Shang B S, Zhang H P, Li Z Z, Zhang Y, Wang G, Liu Y H, Zhao Y, Zhang B, Ke H B, Zhou J H, Bai H Y and Wang W H 2024 *Nat. Mater.* **23** 1193
[10] Drehman A J, Greer A L and Turnbull D 1982 *Appl. Phys. Lett.* **41** 716
[11] Schroers J, Wu Y, Busch R and Johnson W L 2001 *Acta Mater.* **49** 2773
[12] Sanders W S, Warner J S and Miracle D B 2006 *Intermetallics* **14** 348
[13] Wang W H 2007 *Prog. Mater. Sci.* **52** 540
[14] Egami T 1997 *Mater. Sci. Eng. A* **226** 261
[15] Laws K J, Miracle D B and Ferry M 2015 *Nat. Commun.* **6** 8123
[16] Suryanarayana C, Seki I and Inoue A 2009 *J. Non-Cryst. Solids* **355** 355
[17] Lu Z P and Liu C T 2002 *Acta Mater.* **50** 3501
[18] Cheng Y, Ma E and Sheng H 2009 *Phys. Rev. Lett.* **102** 245501
[19] Peng H L, Li M Z, Wang W H, Wang C Z and Ho K M 2010 *Appl. Phys. Lett.* **96** 021901
[20] Long Y, Cao Q P, Wang X L, Xu T D, Su Y, Wang X D, Ding S Q, Zhang D X and Jiang J Z 2022 *J. Alloys Compd.* **907** 164534
[21] Wu B Q, Kong L T and Li J F 2022 *Acta Mater.* **235** 118059
[22] Liu X, Wang S D, Fan H Y, Ye Y F, Wang H, Wu Y and Lu Z P 2018 *Intermetallics* **101** 133
[23] Xi X K, Li L L, Zhang B, Wang W H and Wu Y 2007 *Phys. Rev. Lett.* **99** 095501
[24] Hirata A, Kang L J, Fujita T, Klumov B, Matsue K, Kotani M, Yavari A R and Chen M W 2013 *Science* **341** 376
[25] Wu Z W, Li M Z, Wang W H and Liu K X 2015 *Nat. Commun.* **6** 6035
[26] Wei G Y, Cui J Z, Wang W, Guo X X, Ren J L and Wang W H 2022 *Phys. Rev. Mater.* **6** 055601
[27] Cheng Y Q and Ma E 2011 *Prog. Mater. Sci.* **56** 379
[28] Sheng H W, Luo W K, Alamgir F M, Bai J M and Ma E 2006 *Nature* **439** 419
[29] Li M Z, Wang C Z, Hao S G, Kramer M J and Ho K M 2009 *Phys. Rev. B* **80** 184201
[30] Hao S G, Wang C Z, Li M Z, Napolitano R E and Ho K M 2011 *Phys. Rev. B* **84** 064203
[31] Zhang S, Li Q A, Yang Y and Guan P F 2025 *Chin. Phys. B* **34** 036105
[32] Guan P F, Fujita T, Hirata A, Liu Y H and Chen M W 2012 *Phys. Rev. Lett.* **108** 175501
[33] Sedighi S, Kirk D W, Singh C V and Thorpe S J 2015 *J. Chem. Phys.* **143** 114509
[34] Tang C and Harrowell P 2013 *Nat. Mater.* **12** 507
[35] Hu Y C and Tanaka H 2020 *Sci. Adv.* **6** eabd2928
[36] Zhao R, Jiang H Y, Luo P, Sun Y T, Li Z A, Wu W W, Shen L Q, Liu M, Zhao S F, Wen P, Zhang Q H, Gu L, Bai H Y and Wang W H 2020 *Appl. Phys. Lett.* **117** 131903
[37] Zomorodian A and Carlsson G 2005 *Discrete Comput. Geom.* **33** 249
[38] Otter N, Porter M A, Tillmann U, Grindrod P and Harrington H A 2017 *EPJ Data Sci.* **6** 1
[39] Edelsbrunner H, Letscher J and Zomorodian A 2002 *Discrete Comput. Geom.* **28** 511
[40] Silva V, Ghrist R and Algeb 2007 *Geom. Topo.* **7** 339
[41] Hiraoka Y, Nakamura T, Hirata A and Nishiura Y 2016 *Proc. Natl. Acad. Sci.* **113** 7035
[42] Bendich P, Marron J S, Miller E, Pieloch A and Skwerer S 2016 *Ann. Appl. Stat.* **10** 198
[43] Clough J R, Byrne N, Oksuz I, Zimmer V A, Schnabel J A and King A P 2022 *IEEE Trans. Pattern Anal. Mach. Intel.* **44** 8766
[44] Ghrist R 2008 *Bull. Am. Math. Soc.* **45** 61
[45] Murakami M, Kohara S, Kitamura N, Akola J, Inoue H, Hirata A, Hiraoka Y, Onodera Y, Obayashi I, Kalikka J, Hirao N, Musso T, Foster A S, Idemoto Y, Sakata O and Ohishi Y 2019 *Phys. Rev. B* **99** 045153
[46] Sørensen S S, Biscio C A N, Bauchy M, Fajstrup L and Smedskjaer M M 2020 *Sci. Adv.* **6** eabc2320
[47] Plimpton S 1995 *J. Comput. Phys.* **117** 1
[48] Mendelev M I, Kramer M J, Ott R T, Sordelet D J, Yagodin D and Popel P 2009 *Philos. Mag.* **89** 967
[49] Mishin Y, Mehl M J and Papaconstantopoulos D A 2002 *Phys. Rev. B* **65** 224114
[50] Mendelev M I and King A H 2013 *Philos. Mag.* **93** 1268
[51] Mendelev M I and Ackland G J 2007 *Philos. Mag. Lett.* **87** 349
[52] Mendelev M I, Kramer M J, Becker C A and Asta M 2008 *Philos. Mag.* **88** 1723
[53] Lechner W and Dellago C 2008 *J. Chem. Phys.* **129** 114707
[54] Zomorodian A 2012 *Adv. Appl. Comput. Topol.* **70** 1
[55] Rocks J W, Liu A J and Katifori E 2020 *Phys. Rev. Res.* **2** 033234
[56] Rycroft C H 2009 *Chaos* **19** 041111
[57] Chintakunta H, Gentimis T, Gonzalez-Diaz R, Jimenez M J and Krim H 2015 *Pattern Recognit.* **48** 391
[58] Newman M E 2002 *Phys. Rev. lett.* **89** 208701
[59] Peng H L, Li M Z and Wang W H 2013 *Appl. Phys. Lett.* **102** 131908
[60] Han D, Wei D, Yang J, Li H L, Jiang M Q, Wang Y J, Dai L H and Zaccone A 2020 *Phys. Rev. B* **101** 014113
[61] Cowley J M 1965 *Phys. Rev.* **138** 1384